ELSEVIER

Journal of Power Sources 112 (2002) 606–613

JOURNAL OF POWER SOURCES

www.elsevier.com/locate/jpowsour

Capacity fade of Sony 18650 cells cycled at elevated temperatures Part I. Cycling performance

P. Ramadass, Bala Haran, Ralph White, Branko N. Popov*

Department of Chemical Engineering, University of South Carolina, Columbia SC 29208, USA

Received 2 August 2002; accepted 30 August 2002

Abstract

The capacity fade of Sony 18650 Li-ion cells increases with increase in temperature. After 800 cycles, the cells cycled at RT and 45 °C showed a capacity fade of 30 and 36%, respectively. The cell cycled at 55 °C showed a capacity loss of about 70% after 490 cycles. The rate capability of the cells continues to decrease with cycling. Impedance measurements showed an overall increase in the cell resistance with cycling and temperature. Impedance studies of the electrode materials showed an increased positive electrode resistance when compared to that of the negative electrode for cells cycled at RT and 45 °C. However, cells cycled at 50 and 55 °C exhibit higher negative electrode resistance. The increased capacity fade for the cells cycled at high temperatures can be explained by taking into account the repeated film formation over the surface of anode, which results in increased rate of lithium loss and also in a drastic increase in the negative electrode resistance with cycling.

Keywords: Impedance; Electrode resistance; Electrochemical impedance spectroscopy

1. Introduction

The capacity fade of Li-ion batteries can be attributed to the unwanted side reactions that occur during overcharge which causes electrolyte decomposition, structural changes, passive film formation and active material dissolution [1]. Several other capacity fading mechanism namely complete exfoliation of the electrode material due to solvent co-intercalation [2] and electronic isolation of active mass [3] has also been clearly addressed. Many recent advances in Li-ion batteries have made them good performing cells at temperature range between −30 and +40 °C [4].

Zhang et al. [5] using electrochemical impedance spectroscopy (EIS) studied the capacity fade of commercially available $LiCoO_2$ based Li-ion cells at room temperature. The results indicated that the positive electrode contributes more to the capacity fade with cycling. The capacity loss was attributed to higher impedance of $LiCoO_2$ electrode with cycling due to continuous electrolyte oxidation under overcharging conditions.

Ramadass et al. [6] studied the capacity fade of commercially available spinel based Li-ion cells. They showed that the capacity fade of the cell depends upon the charging rate and on the cut-off potential used to charge the cell and they attributed capacity fade to structural degradation at the cathode and loss of active materials at both electrodes due to electrolyte oxidation.

According to Aurbach et al. [7], the possible reasons for capacity fading in Li-ion batteries upon continuous cycling were, degradation of secondary active material (positive and negative electrode), degradation of the electrolyte solution due to reactions with reactive components in the Li-ion batteries and surface reactions on both electrode surfaces that increase the impedance of the electrodes.

For safe use of Li-ion cells in portable electronics, it is critical to study their performance at temperatures higher than 40 °C. Elevated temperature accelerates the degradation of the battery materials, which causes a decline in capacity and premature cell death. Also, raising the temperature one might cause the onset of thermal runaway to occur, where the cell temperature increases dramatically as a result of reactions at the electrode interface that are exothermic in nature.

Thus our study focuses on estimating the capacity fade of commercial Li-ion cells cycled at high temperatures. We choose Sony 18650 cells with $LiCoO_2$ as the positive electrode material. The objective was to compare the cell

* Corresponding author. Tel.: +1-803-777-7314; fax: +1-803-777-8265.
E-mail address: popov@engr.sc.edu (B.N. Popov).

0378-7753/02/$ – see front matter
PII: S0378-7753(02)00474-3

performance at different temperatures, more specifically at temperatures greater than 25 °C. Part I of this series deals with the cycling performance of Sony 18650 cells at elevated temperatures. The study includes an extensive analysis of discharge behavior and charging characteristics at each temperature, discussions regarding the variation of constant current and constant voltage charging time with cycling, rate capability measurements and impedance studies of full cell and individual electrode materials. Part II extends this work further and deals with quantitative estimation of capacity loss with cycling and temperature. The study includes quantifying the capacity loss to three major factors namely rate capability loss, secondary active material ($LiCoO_2$/carbon) loss and primary active material (Li^+) loss.

2. Experimental

The cycling studies were done for Sony 18650 cells with a rated capacity of 1800 mAh. Table 1 shows the physical characteristics of the cell electrodes. For charging the cells, the conventional constant current–constant voltage (CC–CV) protocol was adopted. A direct current of 1 A is used to charge the cell during the constant current part and the cut-off voltage was set to be 4.2 V. Subsequently, the voltage was held constant at 4.2 V till the current drops to 50 mA. Using this protocol the cell could be completely charged to obtain the nominal capacity. Charge–discharge studies were carried out in the potential range of 2.0–4.2 V. Arbin BT-2000 battery cycler has been used for all cycling studies. The cells were cycled at three elevated temperatures apart from room temperature. The temperatures chosen were 45, 50 and 55 °C.

The cells were cycled continuously up to 800 cycles. Three cycle numbers namely, 150, 300 and 800 were chosen to analyze the cycled cells. Tenny Model T6S environmental chamber was used for cycling studies at elevated temperatures. The chamber is pre-equipped with humidity control and has the capability for operating at temperature range between −40 and 200 °C. Solartron SI 1255 HF Frequency Response Analyzer and Potentiostat/Galvanostat Model 273A were used for the electrochemical characterization of the cycled Sony 18650 cells.

Rate capability studies were performed for the fresh cell as well as for the cycled cells. The cells were charged using the CC–CV protocol followed by discharging at rates in the range between *C*/9 and 1*C*. The cells were left at open circuit for 1 h and after the potential stabilized, the impedance studies were performed. The cell voltage was stable during the experiments and changed <1 mV. Electrochemical impedance spectroscopy (EIS) measurements were done for both, the charged and the discharged states of the battery. The impedance data generally covered a frequency range of 0.01–100,000 Hz. A sinusoidal ac voltage signal of ±5mV was applied.

In order to estimate the impedance of the individual electrodes, the can of cycled Sony 18650 cells were carefully opened at fully discharged state in a glove box filled with ultra pure argon. Next, pellet or disc electrodes were made from the positive and negative electrodes of Sony 18650 cell and were used as working electrodes in the T-cell. Pure lithium metal was used as the counter and as reference electrode. Separator taken from the Sony 18650 cell was used as a separator in the T-cell. The diameter of the pellet electrodes was 1.20 cm. 1 M $LiPF_6$ was used as the electrolyte in a 1:1 mixture of ethylene carbonate (EC), and dimethyl carbonate (DMC). The EIS studies were also done on the T-cells in order to estimate the contribution of the positive and negative electrode on the total impedance of the cell. Impedance was measured for both lithiated and delithiated states. The frequencies of the ac signal ranged from 10 kHz to 5 mHz.

Table 1
Physical characteristics of Sony 18650 lithium ion battery electrodes

Characteristics	Positive $LiCoO_2$	Negative carbon
Mass of the electrode material (g)	13.4	5.7
Geometric area (both sides) (cm^2)	531	603
Loading on one side (mg/cm^2)	28.4	11.9
Thickness of the electrode (μm) (two side coating + current collector)	183	193
Dimensions of the electrode (cm × cm)	48.3 × 5.5	52.9 × 5.7

3. Results and discussions

3.1. Discharge characteristics

The cells were discharged using a constant current of 1 A until the cell potential reaches the cut-off value of 2.0 V. Fig. 1 presents the capacity fade of Sony 18650 cells when cycled at different temperatures. The initial discharge capacities for the cells cycled at elevated temperatures was found to be higher when compared with the cell cycled at RT. For

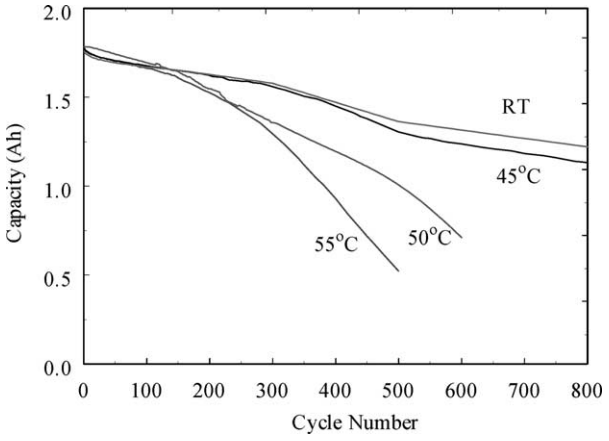

Fig. 1. Discharge capacity of Sony 18650 cells cycled at different temperatures as a function of cycle number.

Table 2
Percentage capacity fade of Sony 18650 cells cycled at different temperatures

Temperature (°C)	Cycle number					
	50	100	150	300	500	800
RT	3.8	5.11	6.09	10.29	22.5	30.63
45	3.8	5.46	7	11.75	26.46	36.21
50	2.4	5.1	7.9	23.9	43.21[a]	–
55	4.3	6.4	9.4	27	70.56	–

[a] Percentage capacity fade after 490 cycles.

the first 150 cycles, all the cells showed similar variation in capacity loss with cycling. However, as shown in Fig. 1 for the cells cycled at 50 and 55 °C a drastic decrease in the capacity is observed within 500 cycles. After 500 cycles, the cells cycled at 50 °C loses about 50% of its rated capacity, while the cells at 55 °C failed to cycle.

Table 2 summarizes the percentage capacity losses with cycling for cells cycled at different temperatures. As shown in Table 2, for the first 100 cycles, the capacity losses were almost the same for all cells. After 150 cycles, there was only a 3% difference in the capacity loss between cells cycled at RT and 55 °C. The cells cycled at RT and 45 °C showed after 800 cycles a capacity fade of 30 and 36%, respectively, after 800 cycles. The cell cycled at 50 °C after 600 cycles showed a capacity loss of 60%, while the cell cycled at 55 °C lost more than 70% of its capacity before it failed to cycle further.

Fig. 2 shows the discharge curves obtained for Sony 18650 cells cycled at different temperatures. Comparing only the discharge profiles of the first cycle, the voltage plateau remains almost identical for all temperatures. The drop in the cell voltage during the beginning of discharge was found to be slightly higher for the cell at RT, whereas for all other temperatures this initial drop was almost the same. As shown in Fig. 2, after 300 cycles, a large drop in the cell voltage was observed for cells discharged at high temperatures.

From the discharge curves, it is seen that the rate of the initial drop in cell voltage and also the capacity fade with cycling are higher for the cells cycled at 50 and 55 °C when compared with other two temperatures. This sudden drop in potential during the initial portion of the discharge curve indicates an increase in the high frequency impedance of the cell (dc resistance). The capacity loss after 300 cycles for the cell cycled at 55 °C was 24%, which is almost double when compared with the capacity loss for the cell cycled at RT.

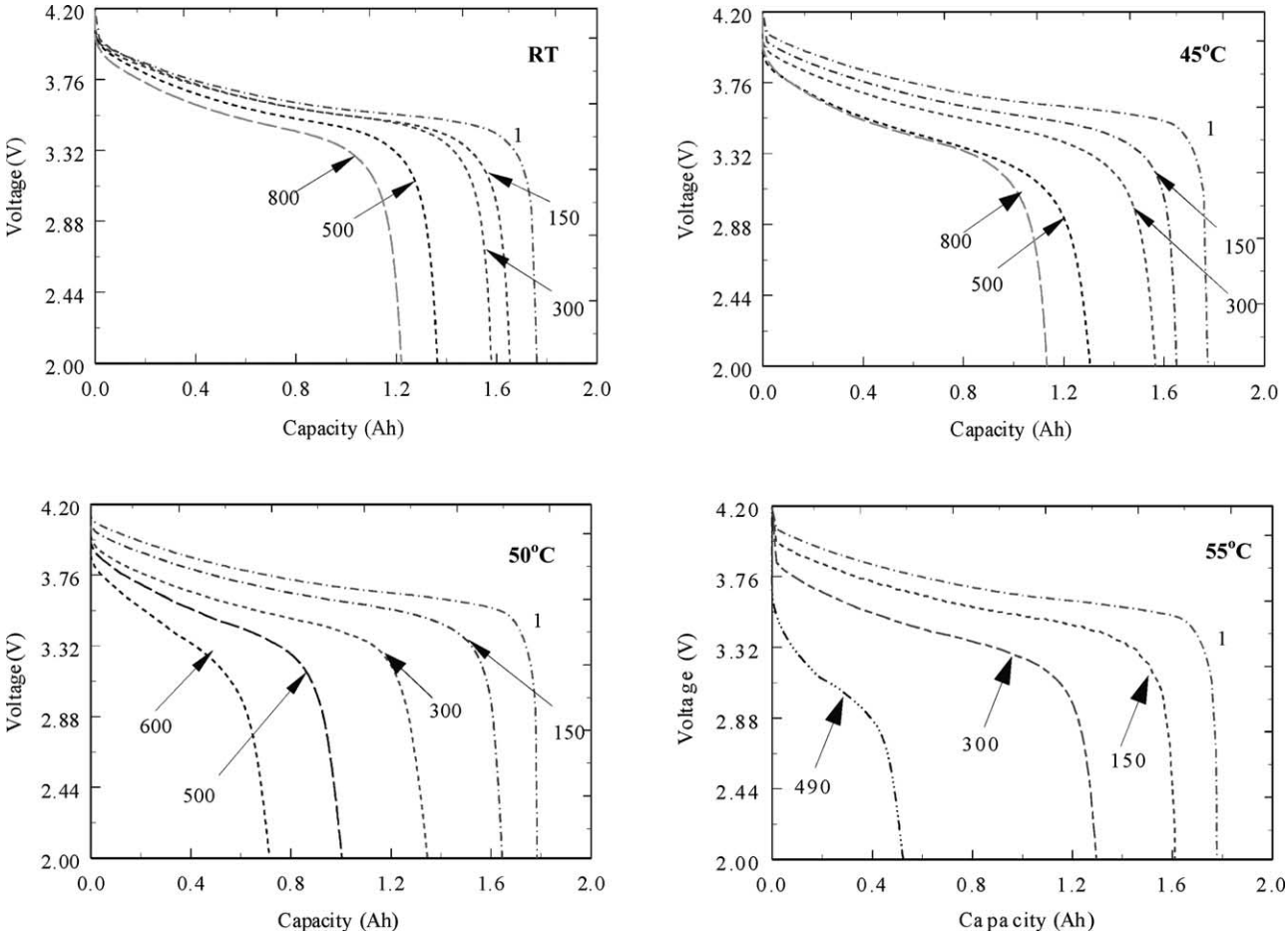

Fig. 2. Discharge curves of Sony 18650 cells cycled at different temperatures for various cycle numbers.

After 500 cycles, the capacity fade for the cell cycled at 55 °C is approximately three times that estimated for the cell cycled at RT. The voltage drop during discharge decreases the energy of the cell drastically. The total energy (E) of a battery during complete charge or complete discharge can be estimated by summation of the product of cell voltage, current (during charge or discharge) and the time of charge/discharge. During charge, the battery is subjected to both constant current and constant voltage. The total energy obtained is a sum of energy expended during these two portions of the charge curve. This can be calculated as

$$E_{\text{CC-chg}} = \sum_i V_i I \Delta t_i \quad (1)$$

$$E_{\text{CV-chg}} = \sum_i V I_i \Delta t_i \quad (2)$$

$$E_{\text{chg}} = E_{\text{CC-chg}} + E_{\text{CV-chg}} \quad (3)$$

where, $E_{\text{CC-chg}}$ is the energy that the battery gains during constant current-charging (1 A) during which the voltage rise is monitored for specific intervals of time. Similarly one can define the energy during constant voltage charge $E_{\text{CV-chg}}$. The term Δt in general is the time interval for logging data for voltage change during constant current charge and current change during constant voltage charge. The summation of energies of both CC and CV charge is the total energy stored in the battery. Similarly, the energy during discharge can be calculated as

$$E_{\text{dchg}} = \sum_i V_i I \Delta t_i \quad (4)$$

Table 3 presents the energies of the cells cycled at different temperatures after a complete charge and discharge of the cells. The ratio of discharge to charge energy is also shown in Table 3 and is defined as the efficiency of the cell to deliver energy. As shown in the table, for the first cycle, the efficiency of the cells cycled at elevated temperatures is higher when compared with those cycled at RT. However, after 800 cycles, for the cells cycled at RT, the cell efficiency decreased only 5% while for the cell cycled at 45 °C the efficiency was decreased by 17%. The cells cycled at 50 and 55 °C showed even higher drop in the efficiencies. The observed decrease in efficiency can be attributed to the cell voltage drop during the initial periods of discharge.

Table 3
Variation of energy with cycling for Sony 18650 cells cycled at different temperatures

Cycling temperature (°C)	Cycle number	Energy (E) (Wh)		$(E_{\text{dchg}}/E_{\text{chg}}) \times 100$
		After charge	After discharge	
RT	1	7.08	6.34	89.6
	500	5.64	4.82	85.4
	800	5.04	4.25	84.3
45	1	7.01	6.53	93.2
	500	5.50	4.41	80.2
	800	5.05	3.87	76.4
50	1	7.17	6.65	92.7
	500	4.25	3.44	80.9
55	1	7.01	6.57	93.7
	490	2.35	1.58	67.2

3.2. Charge characteristics

Fig. 3 presents the charge curves for the cells cycled at different temperatures. A constant current of 1A was used to charge the cell until the cell voltage reaches 4.2 V followed by constant voltage charging until the charging current decreases to 50 mA.

To cycle the cells at room temperature the duration of the total charging time (CC + CV) during initial cycles was approximately 3 h. As shown in Fig. 3, one observes a very small increase in the total charging time with cycling. For batteries cycled at elevated temperatures the total charging time during initial phase of cycling was significantly lower when compared to the total charging time estimated for batteries cycled at room temperature. It was necessary to charge these cells only 2 h and 21 min to obtain the nominal capacity under the same charging protocol.

The constant current charging time was found to be higher for the cells cycled at higher temperatures during the first 200 cycles. With further cycling it is seen that the CC time decreases at higher rate for cells cycled at higher temperatures when compared with cells cycled at RT and 45 °C. This is clearly observed in Fig. 3 for the cells cycled at 50 and 55 °C.

After 300 cycles, the total charging times were almost comparable for all temperatures. There was a 10 min decrease in CC charging time between cycle numbers 150 and 300 for cells cycled at room temperature. The corresponding decreases in CC time for 45, 50 and 55 °C were 14, 29 and 39 min, respectively. The results indicated that the cell after 300 cycles cycled at higher temperatures were almost being charged in CV mode rather than in CC mode. The bar plots shown in Fig. 4 compare both the constant current and constant voltage charging times for the cells cycled at four different temperatures. The cycle numbers are indicated in the plot. For the first cycle, the CC charging time increases with increase in temperature from RT to 50 °C beyond which it started to decrease. The constant voltage charging time decreases with temperature up to 50 °C followed by a slight increase at 55 °C. Overall, for first few cycle numbers, the total charging time was found to be lowest for the cell cycled at 50 °C. As discussed earlier, cells cycled at higher temperatures (50 and 55 °C) showed better performance for the first 200 cycles. As shown in Fig. 4, cells cycled at 50 and 55 °C showed a large decrease in the constant current charging time after 300 cycles. At 55 °C, the cell was almost charged in constant voltage mode after 400 cycles. During the entire 800 cycles of charge and

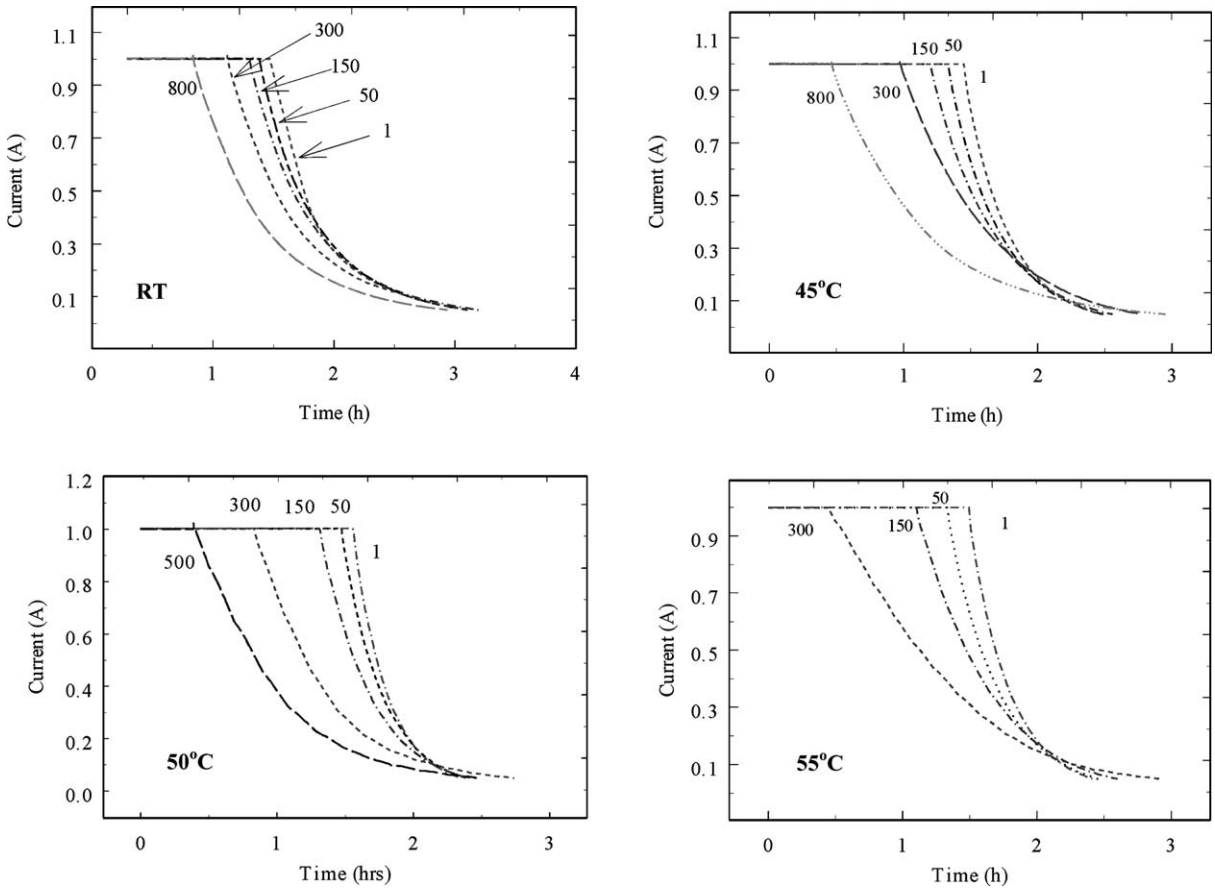

Fig. 3. Charge curves for Sony 18650 cell for several cycles cycled at different temperatures.

discharge, the cells cycled at RT and 45 °C showed a similar trend in terms of decrease in CC time and increase in CV time.

3.3. Rate capability measurements

Rate capability of a Li-ion battery can be defined as the maximum continuous or pulsed output current it can provide. It plays an important role in deciding the cycle life of a Li-ion cell. In general cells having higher rate capability have higher power densities and better cycle life as compared to cells with poor rate capability.

Rate capability studies were performed for fresh cell as well as for the cells cycled at different temperatures. Fig. 5 summarizes the rate capability studies on Sony 18650 cells performed at different temperatures. The tests were done by charging the cells using the same CC–CV protocol as used for cycling studies, where a direct current of 1A was used for CC part. Subsequent to charging, the cells were discharged galvanostatically at discharge rates in the range between *C*/9 and 1*C* rate. These rates correspond to a discharge current of 0.2 and 1.8 A, respectively.

The fresh cell showed only a small decrease in capacity with increase in discharge current indicating that the cell possesses a very good rate capability. The discharge capacity profile looks almost flat with increasing currents up to *C*/2 discharge beyond which the capacity drop was relatively higher for 1*C* rate when compared with other discharge rates. Rate capability measurements after 150 cycles showed a similar decrease in capacity with increasing discharge rates for all temperatures. The rate capability profiles for the cells cycled 150 times look similar to that of the fresh cell for all cycling temperatures. However, after 300 cycles one observes a large difference in the rate of the capacity decay with discharge rate for cells cycled at 50 and 55 °C. For example, the cell cycled to 800 times at 45 °C showed a poor rate capability when compared with that of cell cycled at RT. Similarly, the rate capability continuously diminishes for the cell cycled at 50 °C, which is quite clearly seen in Fig. 5 after 500 cycles.

The variation in the constant current charging time is directly related to the rate capability of the cells, which decreases as the cycle number increases. The observed phenomena may result from a decrease of the Li^+ transference number and increase of resistance for Li-ion intercalation. Transference number of Li^+ decreases due to dissolution of corrosion and reaction products in the electrolyte. Further, corrosion products formed on the surface of both electrodes increase mass transfer limitations for Li^+ intercalation.

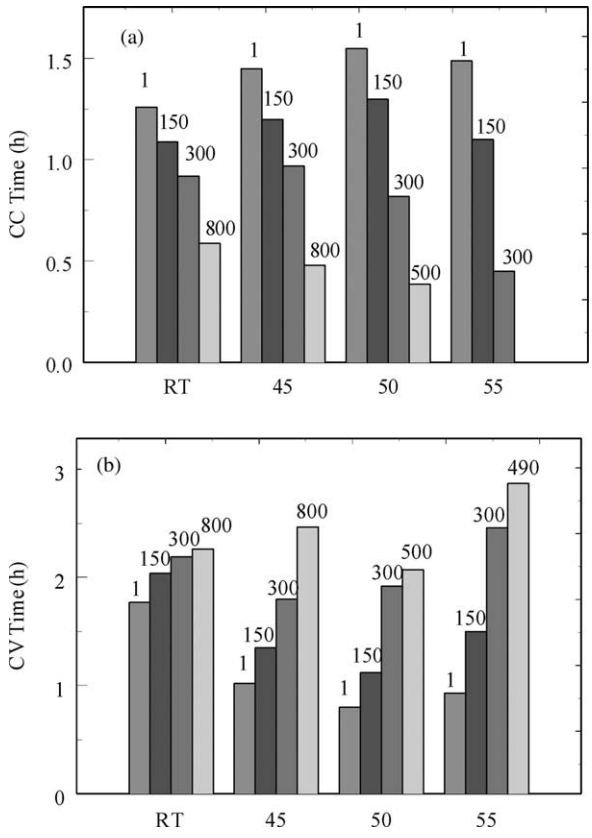

Fig. 4. Variation of constant current (a) and constant voltage (b) charging time with cycle number for Sony 18650 cells.

3.4. Impedance measurements

The increase in the overall battery internal resistance could be obtained by impedance measurements. The cell potential of the Li-ion cell can be represented as

$$V = E_0 - I(R_\Omega + R_P) \quad (5)$$

where E_0 is the equilibrium potential (OCP), I the charging current, R_Ω the electrolyte resistance and R_p the time-dependent and is the sum of cathode and anode resistances.

During initial cycling, the impedance or the overall cell resistance decreases with increase in temperature. The low value of the overall cell resistance for cells cycled at elevated temperatures can be explained by influence of temperature on the processes occurring in the solid phase, at the electrode–electrolyte interface and in the electrolyte. Besides the fact that the conductivity and the diffusion coefficient increase with rise in temperature, it was found that with cycling the overall cell resistance increases with temperature. This could be attributed to two different causes, namely: (i) evaporation of electrolyte, which is accelerated at elevated temperatures and (ii) loss of secondary active material $LiCoO_2$ and carbon and formation of inactive oxides on cathode and thicker interface film on anode due to the side reactions. These products have a larger resistance as compared to the substrate material.

Fig. 6 shows a bar chart that compares the overall cell resistances obtained from impedance measurement for Sony 18650 cells cycled at different temperatures. It is clear from the bar chart, that the internal resistance of the cell cycled at different temperatures is comparable to each other up to 300 cycles. After 800 cycles the overall resistance for the cell at 45 °C is higher than that of the cell cycled at RT. Cells cycled at 50 °C showed even higher impedance after 600 cycles when compared with the impedance of cells cycled 800 times at RT and 45 °C. The resistances of the batteries increases continuously with cycling. Note that the observed increase in resistance is consistent with the variation of capacity fade with cycling. The increased capacity loss after 800 cycles for the cells cycled at 45 °C when compared with cells cycled at ambient conditions can be explained based on increased overall cell resistance.

Similar impedance studies were also done for both positive and negative electrodes of the fresh as well as for the cycled cells. Impedance measurements were carried out for de-lithiated positive electrode and lithiated negative electrode, which would be the actual status of each electrode in a completely discharged full cell. Fig. 7 presents the bar plots that show the comparison of positive and negative electrode resistances obtained from the Nyquist plot for the Sony 18650 cells cycled at different temperatures for different cycle numbers. Impedance measurements taken after 150 cycles show that the electrode resistances almost remain the same for all temperatures with positive electrode resistance being higher than that of negative electrode. With further cycling, the electrode resistances increase with increase in temperature. After 300 cycles we could see that electrode materials taken from the cell cycled at 55 °C showed higher resistance when compared with other temperature. In addition to this, the negative electrode resistance became higher than that of positive electrode for temperatures 50 and 55 °C. The negative electrode resistance continues to remain higher for the cell cycled at 50 °C while for the cells at RT and 45 °C, the positive electrode resistance was high even after 800 cycles. Thus, with continuous cycling of lithium-ion cells, we could observe that the overall cell resistance and the individual electrode resistance go on increasing and this increase is higher when the cells were cycled at elevated temperatures.

In general, capacity fade in lithium-ion cells can be attributed to unwanted side reactions that occur during overcharge or over discharge, that causes electrolyte decomposition, passive film formation, active material dissolution and other phenomena. With continuous cycling of lithium-ion cells, one could observe that the overall cell resistance and the individual electrode resistance increases. This was evident form the impedance measurements for the full cell as well as for the half-cells with positive and negative electrode materials as working electrodes. The factors that cause the resistance to increase continuously with cycling are related

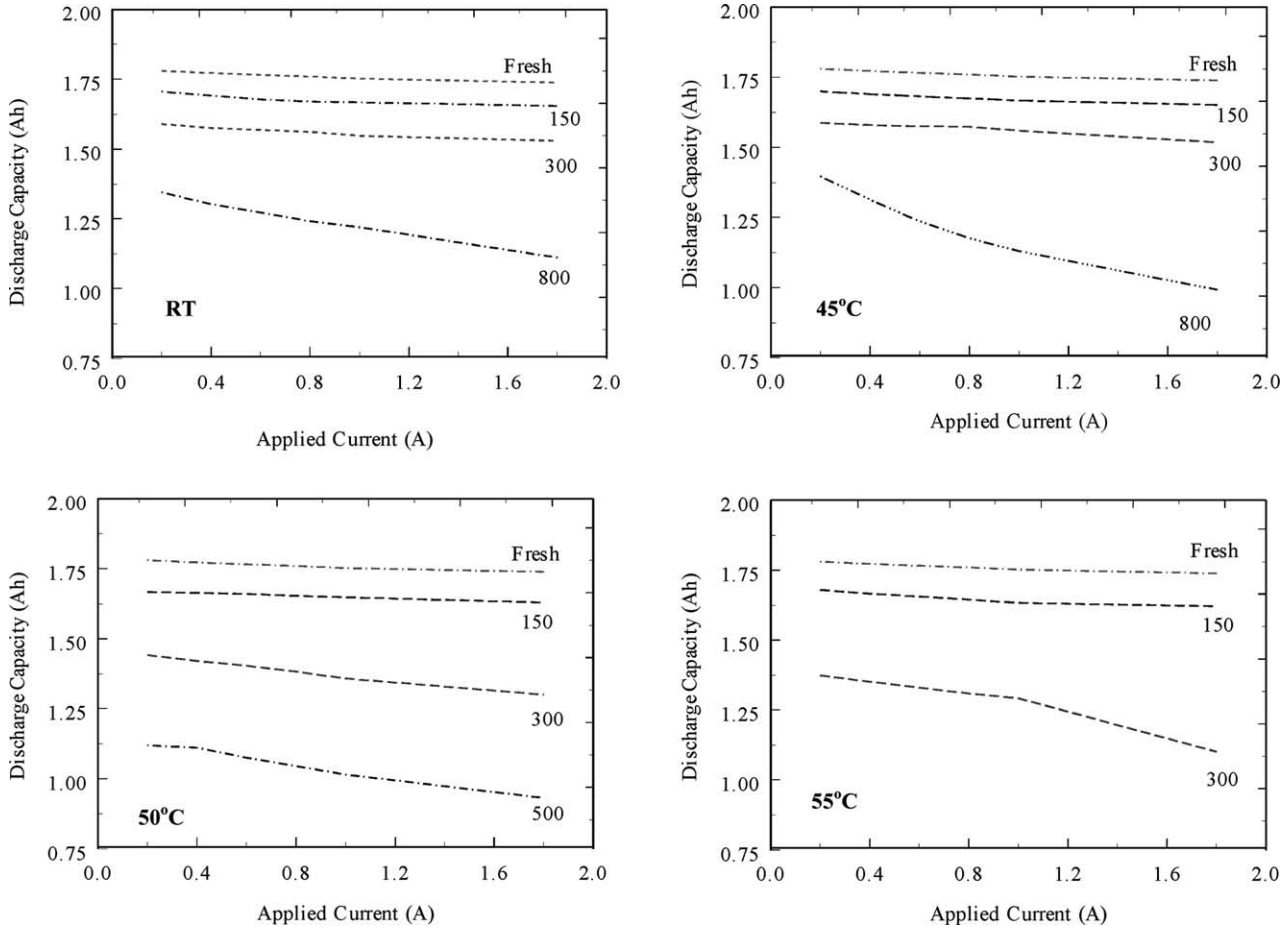

Fig. 5. Rate capability studies for the Sony 18650 cells cycled at different temperatures.

directly to the electrode materials and their interactions with electrolyte. The possible mechanism that could explain the increase in electrode resistance is the formation of thin oxide film, often referred to as the SEI layer that arises due to decomposition of the electrolyte that includes both salt ($LiPF_6$) as well as organic solvent (EC/PC/DMC). At 100% SOC, the positive electrode remains de-lithiated in which case, the presence of metal oxide (CoO_2) is dominated inside the crystal lattice. The transition metal cation Co^{4+} has a strong oxidizing power and can react with the battery electrolyte at the positive electrode–electrolyte interface, which could cause decomposition of the electrolyte to form an oxide film over the positive electrode surface. SEI formation over the surface of the negative electrode during the formation period causes an initial increase in impedance of the Li-ion cell. However, under continuous cycling at normal temperature conditions one observes that the thickness of the SEI layer remains constant and thus the rate of increase in impedance for the negative electrode is lower when compared with that of positive electrode. However, this is not true for cycling under elevated temperatures where a large increase in the negative electrode resistance occurs.

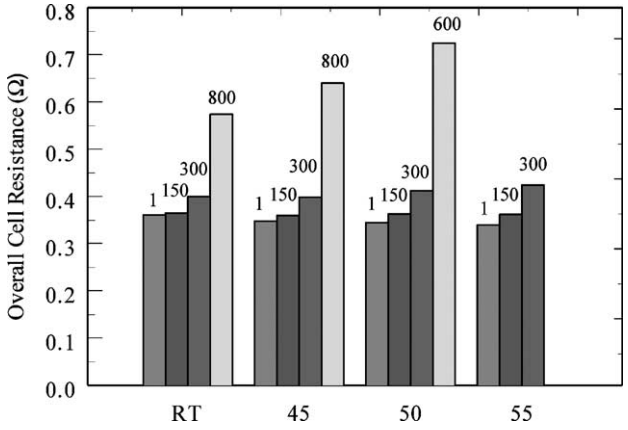

Fig. 6. Comparison of overall cell resistances obtained from impedance measurement for Sony 18650 cells cycled at different temperatures.

The observed increase of the negative electrode resistance explains the higher capacity fade observed for the cells cycled at elevated temperature. The SEI layer formed on a graphite electrode changes in both morphology and chemical composition during cycling at elevated temperature [4]. The R–OCO_2Li phase is not stable on the surface and

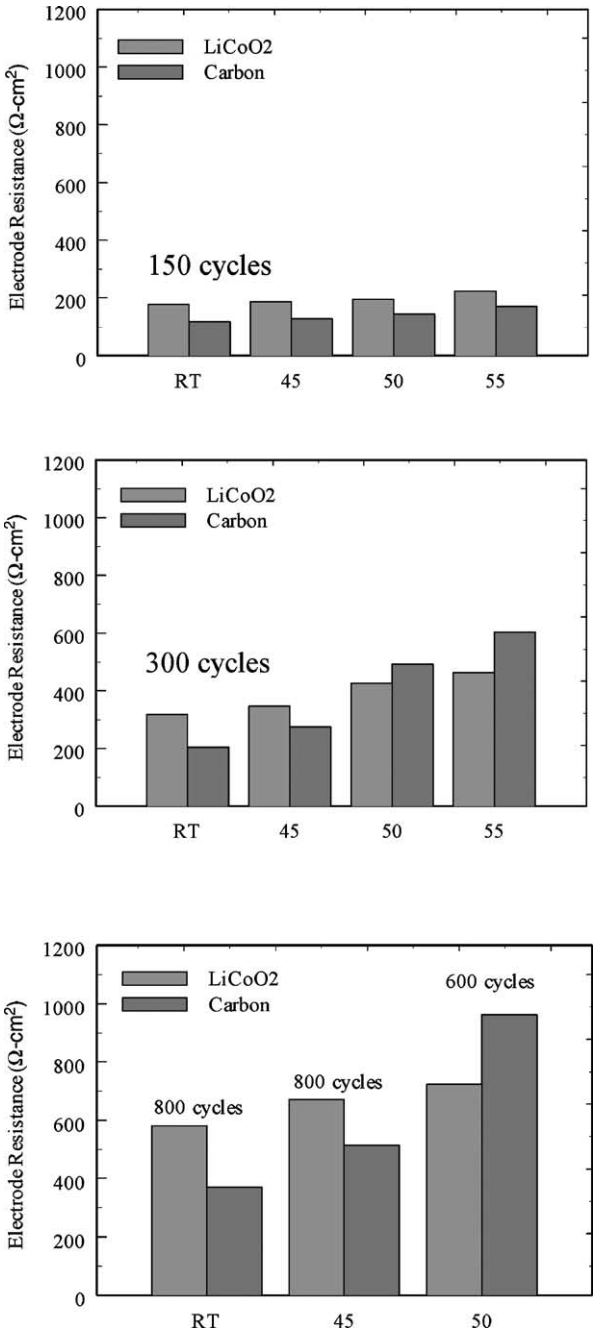

Fig. 7. Comparison of resistances of de-lithiated positive electrode and completely lithiated negative electrode taken from the Sony 18650 cells at cycle numbers 150, 300 and 800 cycled at different temperatures.

decomposes readily when cycled at elevated temperatures (50–55 °C). This creates a more porous SEI layer and also partially exposes the graphite surface, causing loss of charge on continued cycling. SEI and electrolyte (both solvents and salt) decomposition have a more significant influence on the electrochemical performance of graphite electrodes at elevated temperatures.

4. Conclusion

Sony 18650 cells were cycled at different temperatures. It was found that capacity fade of the lithium ion cells increases with increase in cycling temperature. The performance was found to be similar for the first 200 cycles for all cells cycled at different temperatures. Cells cycled at 50 and 55 °C showed an increased rate of capacity loss with increase of the cycle number. The rate capability of the cells continues to decrease with cycling. The impedance measurements for both full and half-cells show an overall increase in the cell resistance with cycling and temperature. Impedance of $LiCoO_2$ always remained higher than that of carbon electrode for the cells cycled at RT and 45 °C. However, for cells cycled at 50 and 55 °C after 200 cycles, the impedance of the negative electrode increases at higher rate than the impedance of the positive electrode. Both primary (Li^+) and secondary active material ($LiCoO_2$) is lost during charging. Thus capacity fade for the cells cycled at elevated temperatures can be quantified as primary active material loss (Li^+), secondary active material ($LiCoO_2$/carbon) loss, and capacity loss due to a decrease in the rate capability of the cell with continued cycling. These losses will be quantified in the second part of this paper. The capacity fade for the cell cycled at 50 and 55 °C can be explained by taking into account the repeated film formation over the surface of anode that results in increased rate of lithium loss and the overall cell resistance at high temperatures.

Acknowledgements

Financial support provided by National Reconnaissance Office for Hybrid Advanced Power Sources no. NRO-00-C-1034 and National Science Foundation Grant no. 0097701 is acknowledged gratefully.

References

[1] P. Arora, R.E. White, M. Doyle, J. Electrochem. Soc. 145 (1998) 3647.
[2] M. Winter, J.O. Besenhard, in: J.O. Besenhard (Ed.), Handbook of Battery Materials (Part III), Wiley, NewYork, 1999, Chapter 5, pp. 283–409.
[3] D. Aurbach, B. Markovsky, M.D. Levi, E. Levi, A. Schechter, M. Moshkovich, Y. Cohen, J. Power Sources 81–82 (1999) 95.
[4] A.M. Andersson, K. Edstrom, J. Electrochem. Soc. 148 (2001) A1100.
[5] D. Zhang, B.S. Haran, A. Durairajan, R.E. White, Y. Podrazhansky, B.N. Popov, J. Power Sources 91 (2000) 122.
[6] P. Ramadass, A. Durairajan, B.S. Haran, R.E. White, B.N. Popov, J. Electrochem. Soc. 149 (1) (2002) A54.
[7] D. Aurbach, B. Markovsky, A. Rodkin, M. Cojocaru, E. Levi, H.J. Kim, Electrochim. Acta 47 (2002) 1899.